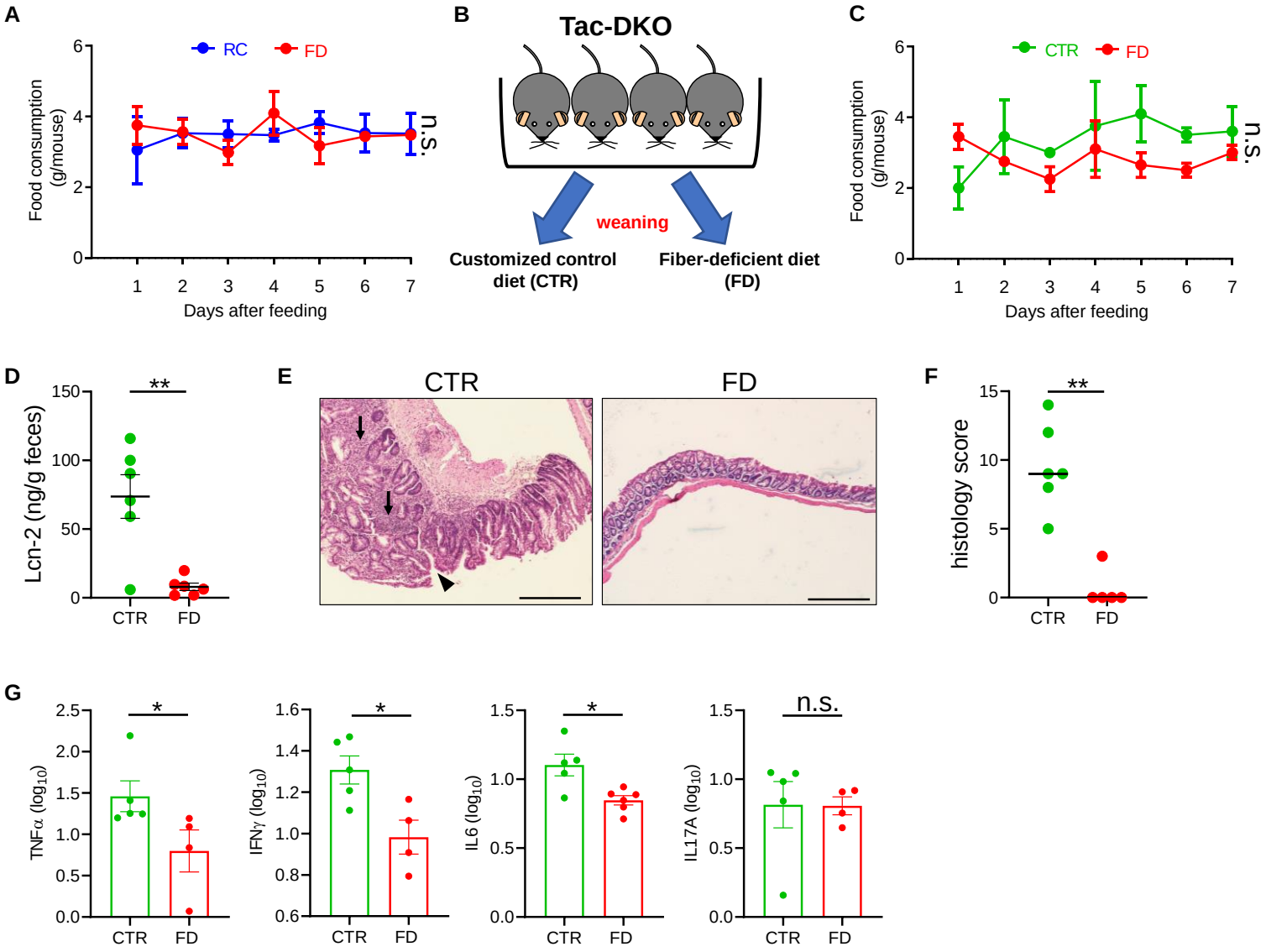

Figure S1. Dietary fiber exclusion prevents intestinal inflammation in Tac-DKO mice fed CTR *vs* FD, Related to Figure 1.

Food consumption in RC- *vs* FD-fed Tac-DKO mice (A) or in CTR- *vs* FD-fed Tac-DKO mice (C). Up to three individual cages/each diet, the amount of food consumed by each animal was calculated. (B) Schematic representation of the experimental design for feeding strategies. (D) Fecal lcn-2 levels in Tac-DKO mice fed either the CTR or the FD mice for 9 weeks (preventive approach). (E) Representative H&E-stained colonic sections from CTR- and FD-fed Tac-DKO mice (preventive approach). Scale bar, 200 µm. Arrowhead shows ulcer. Black arrows indicate colonic transmural inflammation. (F) Histology scores of colonic tissue from CTR-fed Tac-DKO and FD-fed Tac-DKO mice. (H) Gene expression in colonic tissue isolated from CTR-fed Tac-DKO mice and from FD-fed Tac-DKO animals normalized to GAPDH expression.

Each symbol represents one mouse. Data are mean ± SEM (A, C, D and H), or median (F), and representative of two independent experiments, n= 4-6 per group. *p<0.05; n.s. not significant by two-way repeated measures ANOVA followed by Sidak's post-test (A and C), or by two-tailed unpaired t-test (**p=0.0022, D; p=n.s., H), by two-tailed Mann-Whitney U test (**p=0.0043).

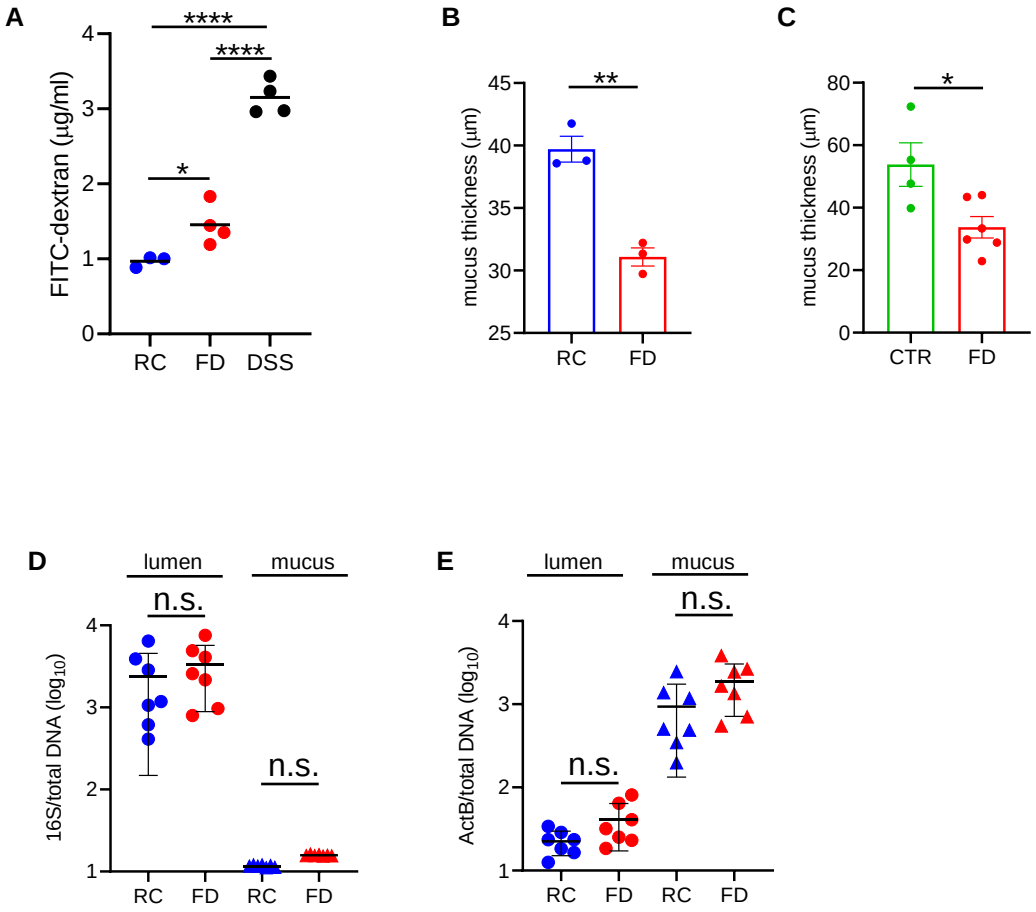

Figure S2. Mucus thickness and intestinal permeability in Tac-DKO mice fed different diets. Bacterial and host genomic copy numbers in Tac-DKO mice fed RC *vs* FD diet, Related to Figure 2.

(A) Intestinal permeability in Tac-DKO mice fed either RC or FD for three weeks (DSS-treated Tac-DKO mice, positive control). Colonic mucus layer measurements in RC-fed *vs* FD-fed Tac-DKO mice (therapeutic approach, B), and CTR-fed *vs* FD-fed Tac-DKO mice (preventive approach, C). Bacterial genome copies (D) and host genomic copy numbers (E) in intestinal luminal and mucus DNA samples isolated from RC-fed or FD-fed Tac-DKO mice.

Each symbol represents one mouse. Data are mean ± SEM (A-C), or mean ± SD (D-E) representative of at least two independent experiments, n= 3-7 per group. *p<0.05; ****p<0.0001; n.s. not significant by one-way ANOVA followed by Tukey's post-test (A), or by two-tailed unpaired t-test (**p=0.0024, B; *p=0.0206, C; p=n.s., D-E).

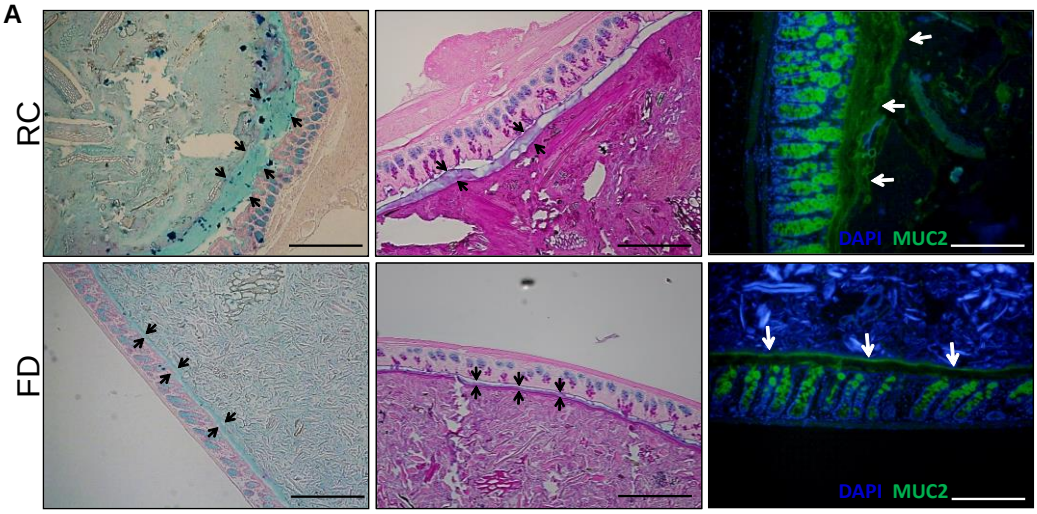
A
RC
FD
DAPI MUC2
DAPI MUC2

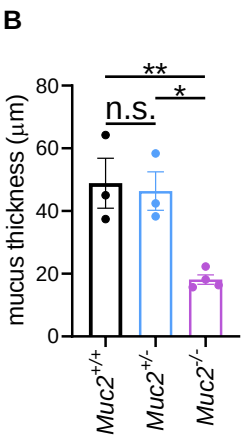
B
mucus thickness (μm)
**
*
n.s.
Muc2+/+
Muc2+/-
Muc2-/-

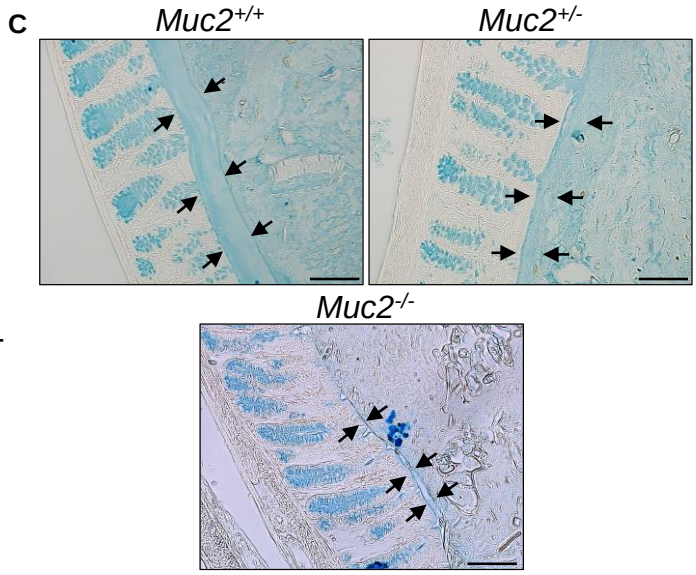
C
Muc2+/+
Muc2+/-
Muc2-/-

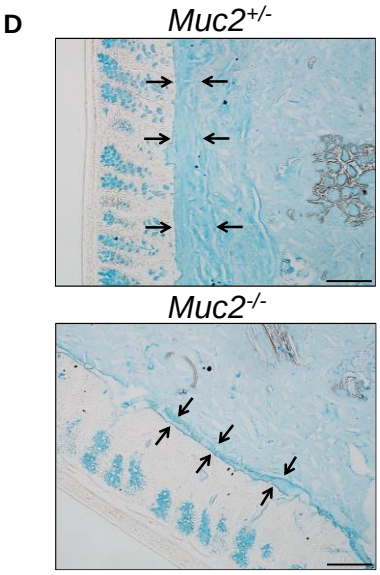
D
Muc2+/-
Muc2-/-

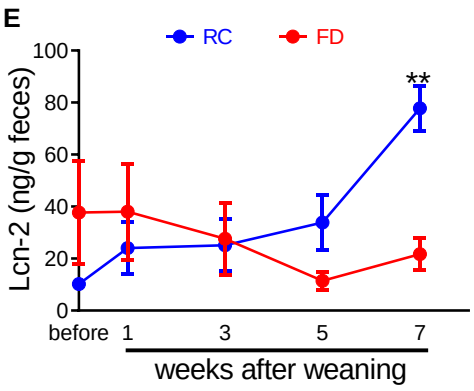
E
RC
FD
Lcn-2 (ng/g feces)
**
before
1
3
5
7
weeks after weaning

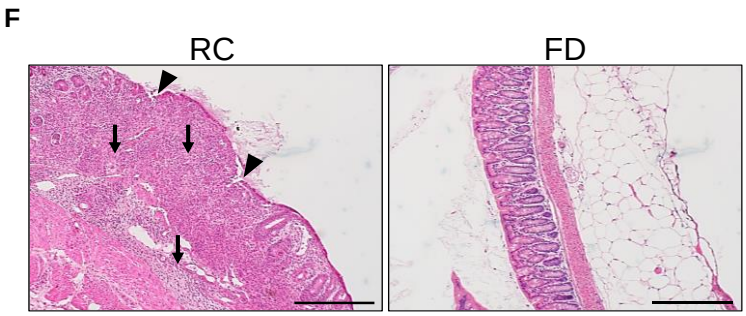
F
RC
FD

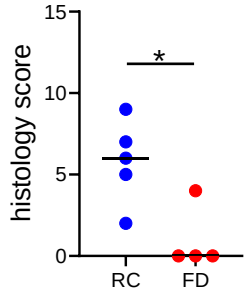
G
histology score
*
RC
FD

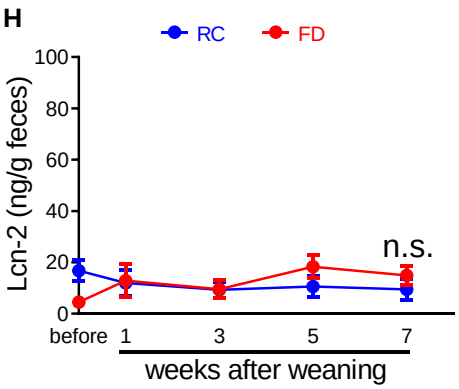
H
RC
FD
Lcn-2 (ng/g feces)
n.s.
before
1
3
5
7
weeks after weaning

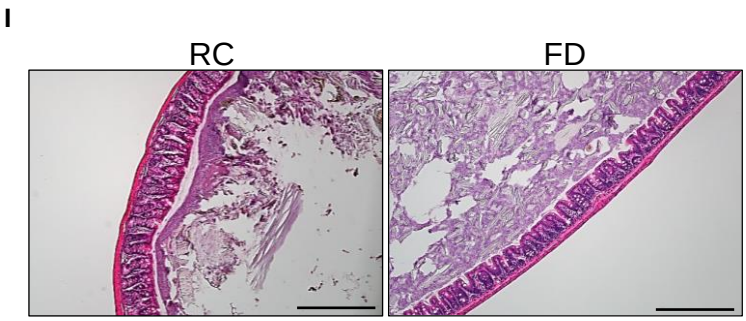
I
RC
FD

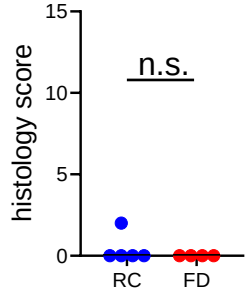
J
histology score
n.s.
RC
FD

Figure S3. Mucus thickness in Jax-DKO mice and Muc2-deficient colony. Lcn-2 levels and histological examination of Jax-DKO and Tac-DKO pups, Related to Figure 3.

(A) Alcian blue-stained (left panel) and Alcian blue/PAS-stained (central panel) colonic sections from *Mucispirillum*-infected Jax-DKO mice fed either the RC (top panels) or the FD diet (lower panels). Opposing black arrows delineate the mucus layer. Scale bars, 200 μm. Immunofluorescence images of colonic sections (right panel) from RC-fed (top panel) or FD-fed (lower panel) Jax-DKO mice stained with anti-Muc2 antibody (green) and DAPI (blue). White arrows indicate the mucus layer. Scale bars, 200 μm. (B) Colonic mucus layer measurements in $Muc2^{+/+}$, $Muc2^{+/-}$ and $Muc2^{-/-}$ mice at steady state. (C) Alcian blue-stained sections of $Muc2^{+/+}$, $Muc2^{+/-}$ and $Muc2^{-/-}$ mice at steady state (C) or 1 day following *Mucispirillum* administration (D). Opposing black arrows delineate the mucus layer. Scale bars, 100 μm. (E) Fecal lcn-2 levels in Tac-DKO pups fed either the RC or the FD . (F) Representative H&E-stained colonic sections from RC- and FD-fed Tac-DKO pups. Scale bar, 200 μm. Arrowhead shows ulcer. Black arrows indicate transmural inflammation. (G) Histology scores of colonic tissue from RC-fed Tac-DKO and FD-fed Tac-DKO mice. (H) Fecal lcn-2 levels in Jax-DKO pups fed either the RC or the FD. (I) Representative H&E-stained colonic sections from RC- and FD-fed Jax-DKO pups. Scale bar, 200 μm. (J) Histology scores of colonic tissues from RC-fed Jax-DKO and FD-fed Tac-DKO mice.

Each symbol represents one mouse. Data are mean ± SEM (B, E and H), or median (G and J), and representative of two independent experiments, n= 3-10 per group. *$p< 0.05$; **$p<0.01$; n.s. not significant by one-way ANOVA followed by Tukey's post-test (B), by two-way repeated measures ANOVA followed by Sidak's post-test (E and H), by two-tailed Mann-Whitney U test (*p=0.0317, G; p=n.s., J).

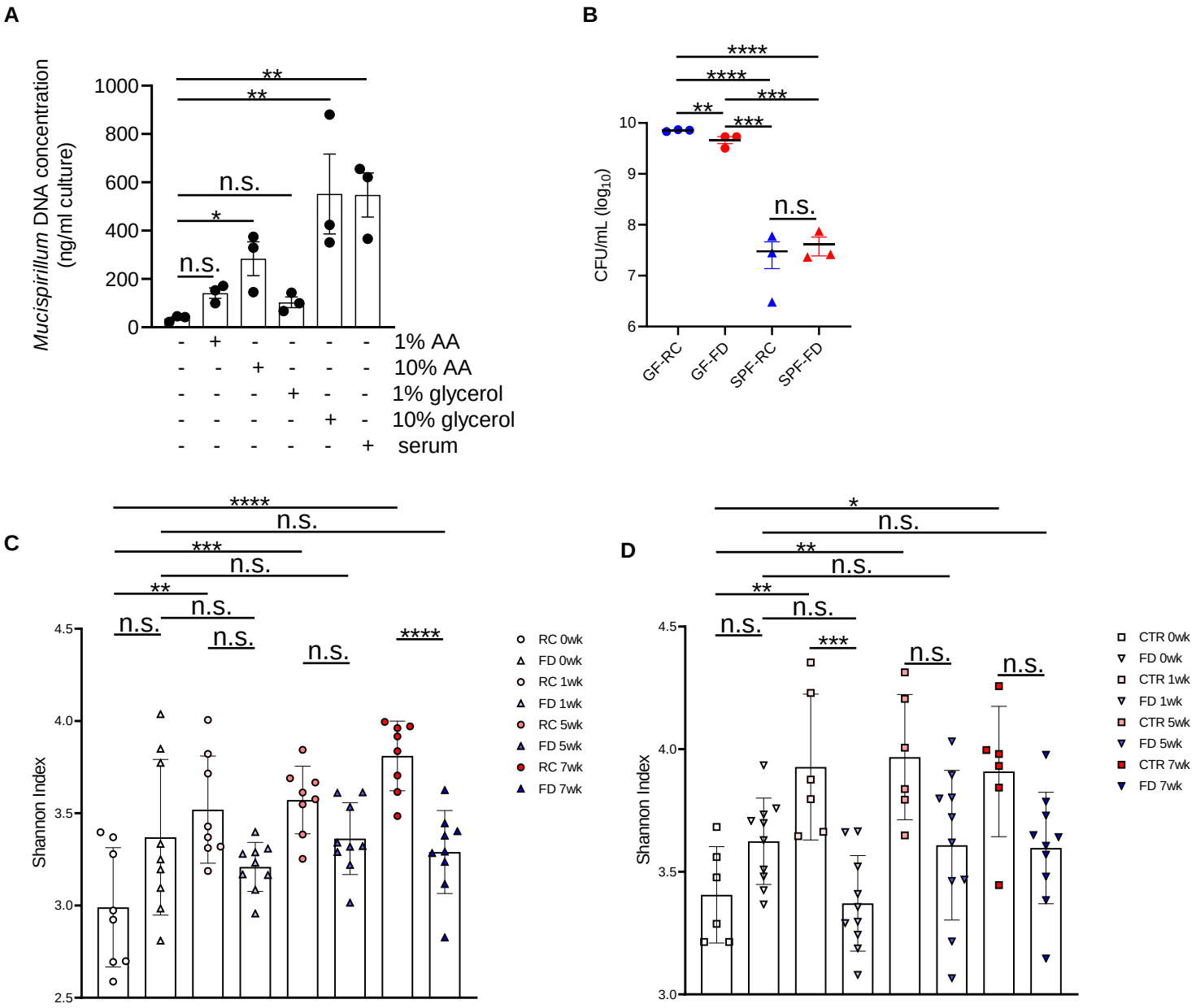

Figure S4. *E. coli* growth in presence of SPF- and GF-derived supernatants, and α diversity in the fecal microbiota of Tac-DKO mice fed different diets, Related to Figure 4.

(A) *Mucispirillum* growth in the presence/absence of amino acids (AA) or glycerol in BHI medium (BHI medium, negative control; BHI medium with serum, positive control) after three days. (B) *E. coli* growth in cecal homogenates derived from SPF or GF mice (RC- or FD-fed) after 24 hours. α diversity of fecal microbiota of Tac-DKO mice (C) or Tac-DKO mice (D).

Each symbol represents one mouse, except for panel B, in which each dot represents data pooled from 3 individual mice. Data are mean ± SEM (A-B), or mean ± SD (C-D), and representative of at least two independent experiments, n= 3-10 per group. *p< 0.05; **p<0.01; ***p<0.001; ****p<0.0001; n.s. not significant by one-way ANOVA followed by Tukey's post-test.

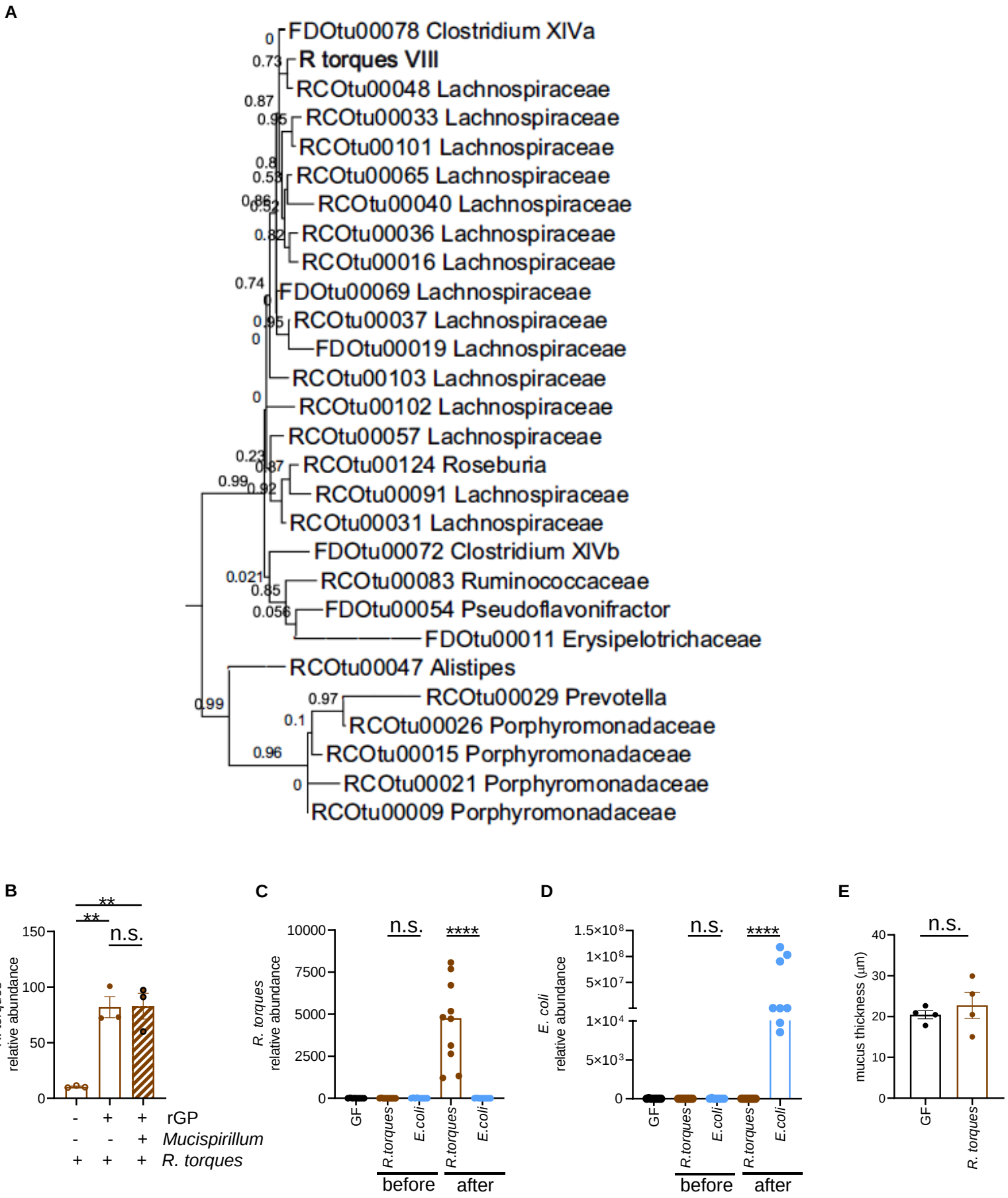
A
FDOtu00078 Clostridium XlVa
R torques VIII
RCOtu00048 Lachnospiraceae
RCOtu00033 Lachnospiraceae
RCOtu00101 Lachnospiraceae
RCOtu00065 Lachnospiraceae
RCOtu00040 Lachnospiraceae
RCOtu00036 Lachnospiraceae
RCOtu00016 Lachnospiraceae
FDOtu00069 Lachnospiraceae
RCOtu00037 Lachnospiraceae
FDOtu00019 Lachnospiraceae
RCOtu00103 Lachnospiraceae
RCOtu00102 Lachnospiraceae
RCOtu00057 Lachnospiraceae
RCOtu00124 Roseburia
RCOtu00091 Lachnospiraceae
RCOtu00031 Lachnospiraceae
FDOtu00072 Clostridium XlVb
RCOtu00083 Ruminococcaceae
FDOtu00054 Pseudoflavonifractor
FDOtu00011 Erysipelotrichaceae
RCOtu00047 Alistipes
RCOtu00029 Prevotella
RCOtu00026 Porphyromonadaceae
RCOtu00015 Porphyromonadaceae
RCOtu00021 Porphyromonadaceae
RCOtu00009 Porphyromonadaceae
B
R. torques relative abundance
n.s.
rGP
Mucispirillum
R. torques
C
R. torques relative abundance
n.s.
****
GF
R.torques
E.coli
before
after
D
E. coli relative abundance
n.s.
****
before
after
E
mucus thickness (µm)
n.s.
GF
R. torques

Figure S5. Phylogenetic tree of microbial species differentially abundant in Tac-DKO mice fed RC vs FD diet. *R. torques* growth in the presence of rectal glycoproteins, and bacterial colonization levels in monocolonized mice, Related to Figure 4.

(A) Phylogenetic tree calculated using the v4 16S rRNA sequences of the microbial species that were more abundant in RC- or FD-fed Tac-DKO mice. *R. torques* VIII was included in the clustering analysis. Numbers indicate phylogenetic distance. *R. torques* was grown in custom chopped meat broth in the presence or absence of rectal glycoproteins (rGP) or *Mucispirillum* for up to three days. (B) *R. torques* abundance was normalized to the universal 16S rRNA gene. Abundances of *R. torques* (C) or *E. coli* (D) in GF mice, in *R. torques*-monocolonized mice and in *E. coli*-monocolonized mice were normalized to the universal 16S rRNA gene. (E) Colonic mucus layer measurements in GF mice and *R. torques*-monocolonized mice.

Each symbol represents one mouse, data are mean ± SEM (E), or median (B-D), and representative of at least two independent experiments, n= 3-10 per group. **p<0.01; ****p<0.0001; n.s. not significant by one-way ANOVA followed by Tukey's post-test (B), by Kruskal-Wallis test followed by Dunn's post-test (C-D), or by two-tailed unpaired t-test (E).

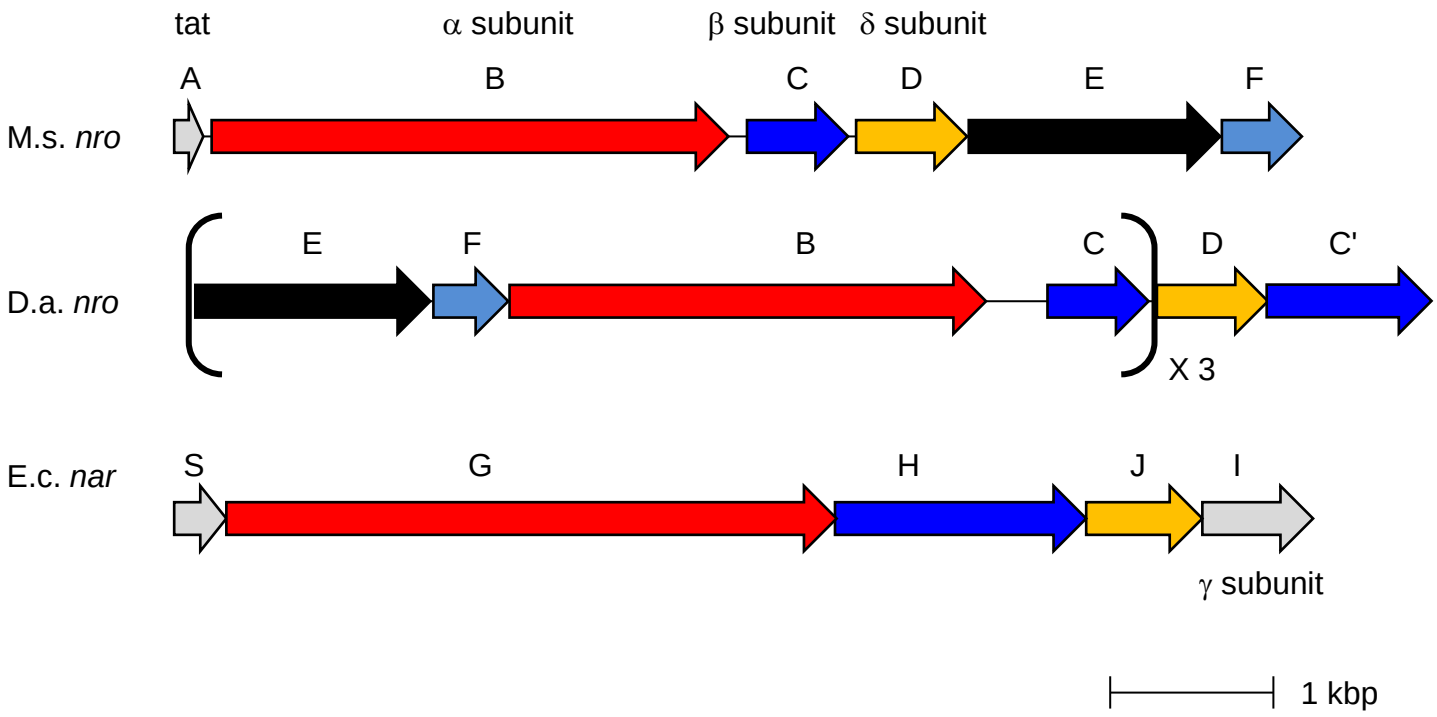

Figure S6. *nro* operon in *Mucispirillum*, Related to Figure 5.

Schematic of putative nitrate reductase operon nro found in *Mucispirillum schaedleri* (M.s.) is shown with the *E. coli* (E.c.) nar operon and the *Denitrovibrio acetiphilus* (D.a.) nro operon as the most homologous operons of *Mucispirillum*-related species. Same colors indicate homologous genes. *D. acetiphilus* has three tandem replicates of *nro*E - *nro*C homologues followed by *nro*D homologues and an additional far-related *nro*C homologue. The locus tag IDs of M.s. *nro*, D.a. *nro* and E.c. *nar* are N508_00422 - N508_00417 (complement) of GCA_000487995, Dacet_0191 - Dacet_0208 of CP001968.1, NarS - NarI of CP009685.1, respectively.

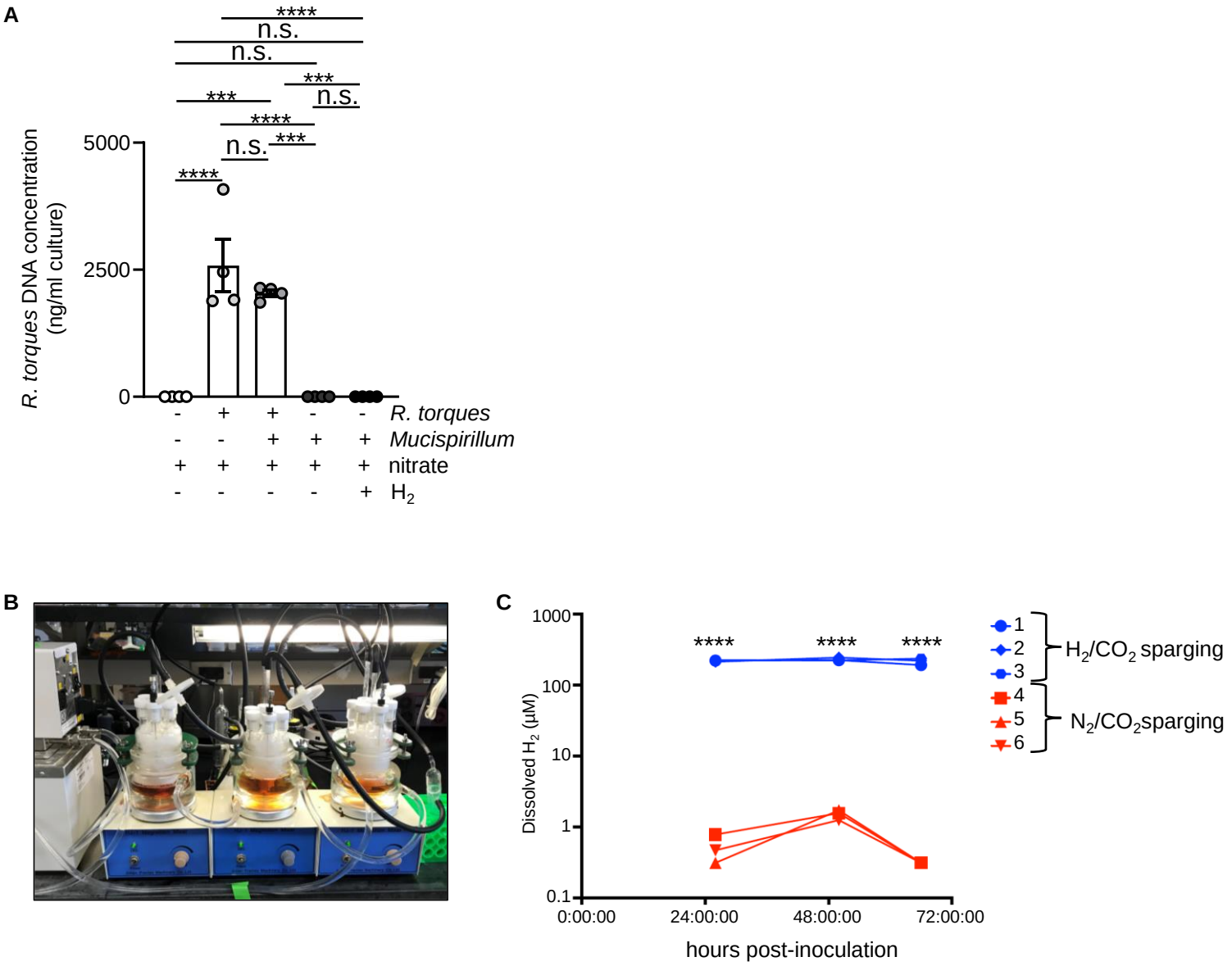

Figure S7. *R. torques* abundance in co-culture experiments with *Mucispirillum* in the absence of exogenous H_2, and concentration of dissolved H_2 in bioreactors, Related to Figure 6.

(A) *R. torques* growth in the presence/absence of *Mucispirillum* in nitrate-supplemented BHI (no exogenous H_2 added) after three days. (B) Photograph of bioreactor vessels operated in batch mode. (C) Dissolved H_2 concentration at 26.5 hours post-inoculation (hpi), 50.5 hpi, and 69.5 hpi. 26.5 hours post-inoculation in either N_2/CO_2 sparged- (n=3) or H_2/CO_2-sparged vessels (n=3).

Each symbol represents one mouse, data are mean ± SEM, and representative of two independent experiments, n= 3-4 per group. ***p<0.001; ****p<0.0001; n.s. not significant by one-way ANOVA followed by Tukey's post-test (A) or by two-way repeated measures ANOVA followed by Sidak's post-test (C).

Name	Sequence 5′-3′	Use	Reference
mouse TNFα qPCR Fw	GCCTCCCTCTCATCAGTTCT	Quantitative PCR of mouse TNFα	(Caruso et al., 2019a)
mouse TNFα qPCR Rv	CACTTGGTGGTTTGCTACGA	Quantitative PCR of mouse TNFα	(Caruso et al., 2019a)
mouse IFNγ qPCR Fw	TCAAGTGGCATAGATGTGGAAGAA	Quantitative PCR of mouse IFNγ	(Caruso et al., 2019a)
mouse IFNγ qPCR Rv	TGGCTCTGCAGGATTTTCATG	Quantitative PCR of mouse IFNγ	(Caruso et al., 2019a)
mouse IL-17A qPCR Fw	GGACTCTCCACCGCAATGA	Quantitative PCR of mouse IL-17A	(Caruso et al., 2019a)
mouse IL-17A qPCR Rv	GGCACTGAGCTTCCCAGATC	Quantitative PCR of mouse IL-17A	(Caruso et al., 2019a)
mouse IL-6 qPCR Fw	CTGCAAGAGACTTCCATCCAGTT	Quantitative PCR of mouse IL-6	(Caruso et al., 2019a)
mouse IL-6 qPCR Rv	AAGTAGGGAAGGCCGTGGTT	Quantitative PCR of mouse IL-6	(Caruso et al., 2019a)
mouse Muc2 qPCR Fw	CCCAGAAGGGACTGTGTATG	Quantitative PCR of mouse Muc2	(Bergstrom et al., 2012)
mouse Muc2 qPCR Rv	TTGTGTTCGCTCTTGGTCAG	Quantitative PCR of mouse Muc2	(Bergstrom et al., 2012)
mouse Muc5ac qPCR Fw	GGTTGTCGATGCAGCCTTGCTT	Quantitative PCR of mouse Muc5ac	(Liu et al., 2021)
mouse Muc5ac qPCR Rv	CCACTTTCTCCTTCTCCACACC	Quantitative PCR of mouse Muc5ac	(Liu et al., 2021)
mouse Tff1 qPCR Fw	CAGGCCCAGGCCCAGGAAGA	Quantitative PCR of mouse Tff1	https://www.origene.com/catalog/gene-expression/qpcr-primer-pairs/mp217526/tff1-mouse-qpcr-primer-pair-nm_009362
mouse Tff1 qPCR Rv	CTGTCATCAAAACAGCAACCTCTC	Quantitative PCR of mouse Tff1	https://www.origene.com/catalog/gene-expression/qpcr-primer-pairs/mp217526/tff1-mouse-qpcr-primer-pair-nm_009362
mouse Tff3 qPCR Fw	CTCTGTCACATCGGAGCAGTGT	Quantitative PCR of mouse Tff3	(Bergstrom et al., 2012)
mouse Tff3 qPCR Rv	TGAAGCACCAGGGCACATT	Quantitative PCR of mouse Tff3	(Bergstrom et al., 2012)
mouse KLF3 qPCR Fw	CCTCTCATGGTTTCCTTGTCGG	Quantitative PCR of mouse KLF3	https://www.origene.com/catalog/gene-expression/qpcr-primer-pairs/mp207224/klf3-mouse-qpcr-primer-pair-nm_008453
mouse KLF3 qPCR Rv	CCTCTGTGGTTCAATTCCAGGC	Quantitative PCR of mouse KLF3	https://www.origene.com/catalog/gene-expression/qpcr-primer-pairs/mp207224/klf3-mouse-qpcr-primer-pair-nm_008453
mouse-GAPDH qPCR Fw	CACCATCTTCCAGGAGCGAG	Quantitative PCR of mouse GAPDH	(Caruso et al., 2019a)

mouse-GAPDH qPCR Rv	GCCTTCTCCATGGTGGTGAA	Quantitative PCR of mouse GAPDH	(Caruso et al., 2019a)
mouse- Actin qPCR Fw	CTCTCAGCTGTGGTGGTGAA	Quantitative PCR of mouse *Actin*	(Chen et al., 2021)
mouse- Actin qPCR Rv	AGCCATGTACGTAGCCATCC	Quantitative PCR of mouse *Actin*	(Chen et al., 2021)
*Mucipirillum nro*A qPCR Fw	AGAAAGCTCAGTATCAAGGCGT	Quantitative PCR of *Mucispirillum nro*A	This study
*Mucipirillum nro*A qPCR Rv	CTGCCATCTTTAGAGCAGCCAT	Quantitative PCR of *Mucispirillum nro*A	This study
*Mucipirillum nro*B qPCR Fw	ATCATGGGGGCAGACTGGTG	Quantitative PCR of *Mucispirillum nro*B	This study
*Mucipirillum nro*B qPCR Rv	GCAGGGCTGCTTGGAACATC	Quantitative PCR of *Mucispirillum nro*B	This study
*Mucipirillum nro*C qPCR Fw	GCCGCATGCTCACAAAATGC	Quantitative PCR of *Mucispirillum nro*C	This study
*Mucipirillum nro*C qPCR Rv	TGAGTGGCAGCAAATGGACA	Quantitative PCR of *Mucispirillum nro*C	This study
*Mucipirillum nro*D qPCR Fw	TCAACAGTCAAGGGAACAGGTG	Quantitative PCR of *Mucispirillum nro*D	This study
*Mucipirillum nro*D qPCR Rv	GCTCATAGGCAATAAAGTCTTCTGG	Quantitative PCR of *Mucispirillum nro*D	This study
*Mucipirillum nro*E qPCR Fw	TATACGGCGGTCTGCCTGTC	Quantitative PCR of *Mucispirillum nro*E	This study
*Mucipirillum nro*E qPCR Rv	GCCTCTGGCAGTATGGGTGT	Quantitative PCR of *Mucispirillum nro*E	This study
*Mucipirillum nro*F qPCR Fw	CCATGCCCGAGCAGGATTTG	Quantitative PCR of *Mucispirillum nro*F	This study
*Mucipirillum nro*F qPCR Rv	TCACAGTATGCAGAGCACCTGA	Quantitative PCR of *Mucispirillum nro*F	This study
*Mucipirillum ubi*D qPCR Fw	CGCAGGGAAGGTCCTTTTGG	Quantitative PCR of *Mucispirillum ubi*D	This study
*Mucipirillum ubi*D qPCR Rv	GCAGTCTTCCATAGGCGGCTT	Quantitative PCR of *Mucispirillum ubi*D	This study

Mucipirillum nth qPCR Fw	AGTGCCGGGGATGGTTGTAG	Quantitative PCR of *Mucispirillum nth*	This study
Mucipirillum nth qPCR Fw	TGCCAAACAGCACAAGCTGA	Quantitative PCR of *Mucispirillum nth*	This study
Mucipirillum gap qPCR Fw	CCCTGCTAATCTTCCTTGGGCTA	Quantitative PCR of *Mucispirillum gap*	This study
Mucipirillum gap qPCR Rv	TGGGTCTGTTGCTGGTGCAG	Quantitative PCR of *Mucispirillum gap*	This study
Mucipirillum qPCR Fw	TCTCTTCGGGGATGATTAAAC	Quantitative PCR of *Mucispirillum*	(Gomes-Neto et al., 2017)
Mucipirillum qPCR Rv	AACTTTTCCTATATAAACATGCAC	Quantitative PCR of *Mucispirillum*	(Gomes-Neto et al., 2017)
R. torques VIII qPCR Fw	TCTAGAGTGCTGGAGAGGTAAG	Quantitative PCR of *R. torques* VIII	This study
R. torques VIII qPCR Rv	GGGATGTCAAGAGCAGGTAAG	Quantitative PCR of *R. torques* VIII	This study
E. coli qPCR Fw	GAGTAAAGTTAATACCTTTGCTC ATTG	Quantitative PCR of *E. coli*	(Kitamoto et al., 2020)
E. coli qPCR Rv	GAGACTCAAGCTKRCCAGTATCA G	Quantitative PCR of *E. coli*	(Kitamoto et al., 2020)
A. muciniphila qPCR Fw	AGAGGTCTCAAGCGTTGTTCGG AA	Quantitative PCR of *A. muciniphila*	(Seregin et al., 2017)
A. muciniphila qPCR Rv	TTTCGCTCCCCTGGCCTTCGTGC	Quantitative PCR of *A. muciniphila*	(Seregin et al., 2017)
Bacterial 16S (8F) qPCR Fw	AGAGTTTGATCCTGGCTCAG	Quantitative PCR of bacterial 16S (*in vivo* studies)	(Caruso et al., 2019a)
Bacterial 16S (338R) qPCR Rv	TGCTGCCTCCCGTAGGAGT	Quantitative PCR of bacterial 16S (*in vivo* studies)	(Caruso et al., 2019a)
Bacterial 16S (341F) qPCR Fw	CCTACGGGAGGCAGCAG	Quantitative PCR of bacterial 16S (*in vitro* studies)	(Chen et al., 2021)
Bacterial 16S (518R) qPCR Rv	ATTACCGCGGCTGCTGG	Quantitative PCR of bacterial 16S (*in vitro* studies)	(Chen et al., 2021)

Table S7. Primers used in this study, Related to Figures 1 to 6, to Figures S1, S2, S3, S4 and S7, Star Methods.